20th Australasian Fluid Mechanics Conference
Perth, Australia
5-8 December 2016

Performance Comparison of Distributed Injection Methods for Hypersonic Film-Cooling

K.D. Basore[1], M. Selzer[2], V. Wheatley[1], R.R. Boyce[3], D.J. Mee[1], B.R. Capra[4], M. Kuhn[2], S. Brieschenk[1]

[1]School of Mechanical & Mining Engineering
University of Queensland, St Lucia, QLD 4072, Australia

[2]Institute of Structures and Design
DLR, Stuttgart, Germany

[3]University of New South Wales at the Australian Defence Force Academy
Canberra, ACT 2600, Australia

[4]Queensland University of Technology
Brisbane, QLD 4000, Australia

Abstract

Film-cooling is one of the promising technologies proposed to help mitigate the heat-transfer load experienced by hypersonic vehicles. To investigate this phenomena, fundamental testing of three different distributed Boundary-Layer (BL) injection methods was carried out in the T4 Stalker Tube using hydrogen injectant. A flat plate model was tested, using a cross-flow of air, at Mach 7.6; a dynamic pressure of 48 kPa; and a flight enthalpy of Mach 10. This fundamental testing was done to help characterize the performance and injection characteristics of different distributed injection methods. The three different injectors selected for this study were a porous Carbon/Carbon (C/C) Ceramic-Matrix-Composite (CMC); a porous oxygen compatible CMC; and a Multi-Port Injector Array (MPIA) optimised for scramjet conditions. Of these, the C/C CMC performed the best, overall, when examining the heat-transfer reduction for both a laminar and transitional-turbulent BL in a hypersonic cross-flow.

Introduction

Surviving the heat-transfer loads within a hypersonic vehicle flight envelope has been identified as one of the main technical roadblocks currently associated with sustained hypersonic flight [6]. Distributed injection film-cooling technologies, originally tested in the 1970s, have previously been used to try to reduce the heat transfer to these types of vehicles but have not had widespread use due to the limitations at the time [9, 10]. Recent developments in the production of porous CMCs as well as the optimization of dense small port-hole injector arrays has led to the current systematic study on the performance characteristics of these different distributed injection methods. Three different injectors were chosen to be examined for this study.

Shown in Fig. 1, the injectors chosen for this study are a fibre embedded C/C Melt Infiltration (MI) intermediary CMC from the DLR Stuttgart [11]; a naturally porous alumina-zirconia oxide CMC [4]; and an MPIA optimized for the best film-cooling performance in a scramjet combustor as defined in [8].

For brevity, only the individual results for the C/C CMC are presented along with the final comparison for all three injectors at the two chosen fuelling rates.

Experimental Model

To enable this fundamental investigation of distributed injection into a hypersonic cross-flow, a flat plate was designed to be able to incorporate the different injectors, as well as different leading edges, in order to test the injectors for both laminar and transitional-turbulent BLs. Figure 2 shows the model in the T4 test section and some of the key design features. Figure 3 shows a schematic of the sensors that were used in the testing. For simplicity only the Thin-Film Heat-transfer Gauge (TFHG) data is presented in this paper.

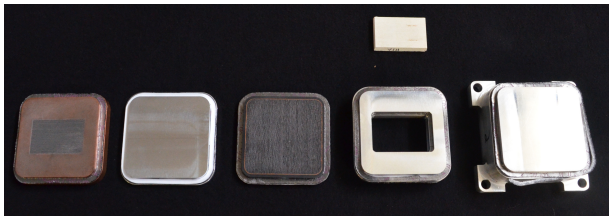

Figure 1. Injection inserts from left to right: copper encased oxy-CMC; MPIA; C/C CMC; oxy-CMC; and the laminar baseline.

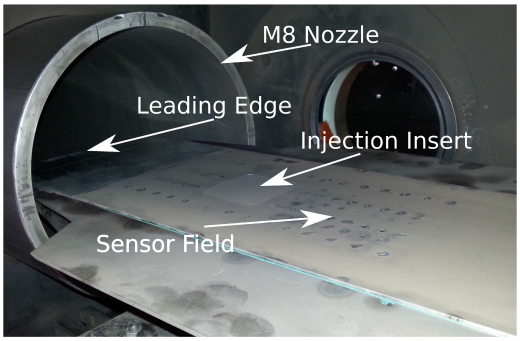

Figure 2. Model in the T4 test section.

To achieve a transitional-turbulent BL by the injection location, boundary layer trips from the design methodology of [1] with a k/δ from the X-33 criteria of [2] were used. This design methodology has previously been validated in the T4 facility for the approximate tripped transition point as well as the associated hypersonic delay [12]. Figure 4 shows an overview of the design of the trips used.

Table 1 shows the experimental flow conditions which were based on the 48 kPa dynamic pressure, Mach 10 enthalpy scramjet flight trajectory of [7]. This tunnel condition was chosen due to its reasonable approximation to the conditions seen on the forebody of a Mach 10 scramjet.

To define the effect the coolant mass-flow rate had, two different equivalence ratios, ϕ, were examined. As there was no definable capture area for the flat plate, the extrapolated circumferential area from the triple-ramp scaled SCRAMSPACE

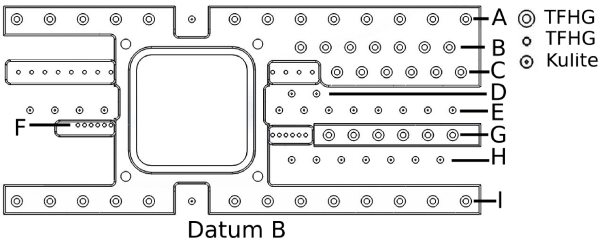

Figure 3. Sensor placement on the model.

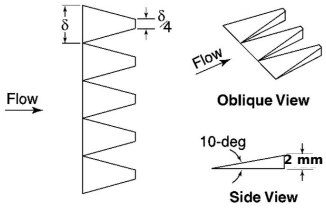

Figure 4. X-43A trip 2c design used for this testing. Adapted from [1].

HEG inlet was used at the equivalent leading edge distance as measured on the experimental model [3]. This extrapolation assumes that the distributed injection would occur around the entire circumference of the axisymmetric engine and gives context to the necessary plenum pressure for each of the injectors. The low momentum fuel injection case was defined as $\phi \approx 0.1$ and the high momentum as $\phi \approx 0.5$.

C/C CMC Results

As a reference to the different injectors, a smooth metal insert was used to establish the baseline heat-transfer levels for the model (Fig. 1). For clarity, these baseline levels are only displayed for the C/C CMC and not for the multiple injector comparisons following. The baseline comparisons are presented here to highlight the level of film-cooling that was achieved when compared to the heat-transfer levels experienced for no injection. All the heat-transfer rates are presented in the non-dimensionalized modified Stanton number shown in Eq 1 with a previous, comparable, calculated uncertainty on these type of measurements being $\pm 18\%$ [12].

$$s_t = \frac{Q_W}{\rho_\infty u_\infty \left(H_0 - C_p T_W\right)} \tag{1}$$

Where, ρ_∞ is the nozzle exit density; Q_W is the heat transfer into the wall; C_p is the constant pressure specific heat; and T_W is the wall temperature (assumed to be 300 K in impulse facilities).

Laminar

When the flat plate model was configured without the BL trips and the shorter leading edge, the baseline heat-transfer levels in Fig. 5 shows how, when compared to the theoretical level [5], that a laminar BL was established over the model. The resulting BL height (δ_{99}) at the injection location was ≈ 1.69 mm.

Figure 5 also displays the film-cooling effect behind the sample for both the high and low momentum injection cases and how the high momentum has a larger cooling effect for a much longer distance downstream.

The mean, relative, reduction in heat transfer for the low momentum and high momentum cases 80 mm behind the injection sample were 10.4% and 77.7% respectively.

Freestream Mach Number	M_∞	7.40	Non
Flow Total Enthalpy	H_0	4.46	MJ/kg
Static Temperature	T_∞	391	K
Static Pressure	p_∞	4.18	kPa

Table 1. T4 nozzle exit conditions

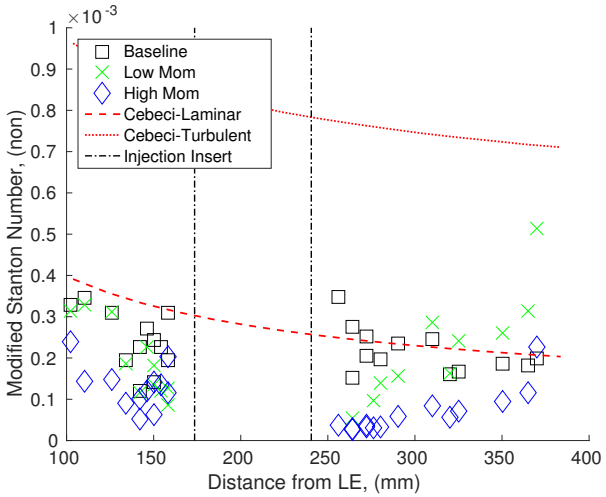

Figure 5. C/C: laminar. T4 shots in order: 11904, 11903, and 11902

Turbulent

The comparative transitional-turbulent heat-transfer level that was achieved by the injection location from utilising the BL trips and longer model leading edge can be seen as the baseline in Fig. 6.

Again, the high momentum injection results in a larger cooling effect with the mean relative reduction 80 mm behind the injection location being 86.1% when compared to 46.7% for the low momentum case. It is interesting to note that the high momentum case reduces the heat-transfer by less than that seen for the laminar BL (Fig. 5) even though it is from a turbulent heating level.

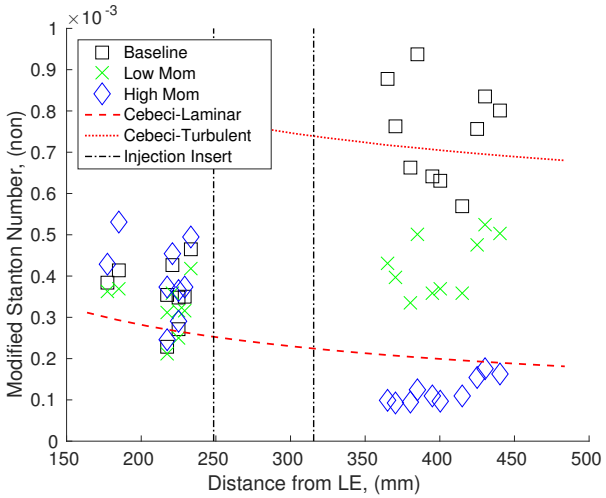

Figure 6. C/C: transitional-turbulent. T4 shots in order: 11917, 11916, and 11915

Laminar-Turbulent Comparison

Examining Fig. 7 as well as the pre-injector Stanton number

readings in both Fig. 5 and 6, it can be seen that the C/C CMC injector separated the upstream flow for the laminar BL but not, to any measurable extent, for the transitional-turbulent case. This flow separation was seen for all the injectors tested and varied in size according to the injection method used.

In examining the relative difference between the laminar to turbulent high momentum cases, the mean post-sample Stanton number only rose 4.44×10^{-5} while the mean uncooled post-sample baseline rose 5.78×10^{-4}. Comparing these uncooled to cooled differentials results in a ratio of 0.078:1. This small relative, as well as absolute, change for the high momentum injection shows that for this particular flow, the competing effects of the enhanced mixing for the turbulent case, and the flow separation and lower maximum heat-transfer for the laminar case, displays an insensitivity of the resulting film-cooling effectiveness to the state of the boundary layer.

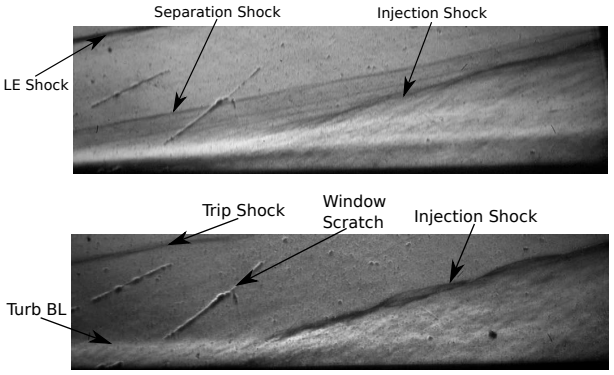

Figure 7. Schlieren comparison on injection induced separation. Shot 11902 & 11915.

Comparison Results

Laminar - Low Momentum

Figure 8 shows that the C/C performs marginally better than the MPIA in both the magnitude of the Stanton number reduction and in the downstream-extent of the cooling effect. The oxy-CMC has a very small section of cooling before transitioning the flow to a turbulent level almost by the end of the sensor field. The Stanton numbers are also higher in the separated region upstream of the injector for the oxy-CMC than for either the C/C or the MPIA.

Laminar - High Momentum

Figure 9 shows the Stanton numbers for the laminar high-momentum case. This figure shows that the C/C performs better than the MPIA in both the downstream-extent and level of heat-transfer reduction. Injection from the oxy-CMC again transitions the flow but the Stanton number remains lower than those seen in Fig. 8.

Turbulent - Low Momentum

In Fig. 10, the C/C CMC and the MPIA display similar levels of cooling as well as a similar downstream-extent. Also, it can be seen that the Stanton number readings upstream of the injector for the MPIA and C/C are at a similar elevated level highlighting the lack of influence these injectors have upstream of the injection location. Interestingly, the oxy-CMC has a slightly higher reading for the pre-injection Stanton number which is, currently, being assumed to be a combination of gauge drift and tunnel condition variation as the schlieren flow visualisation and measured pressure data do not show any measurable separation

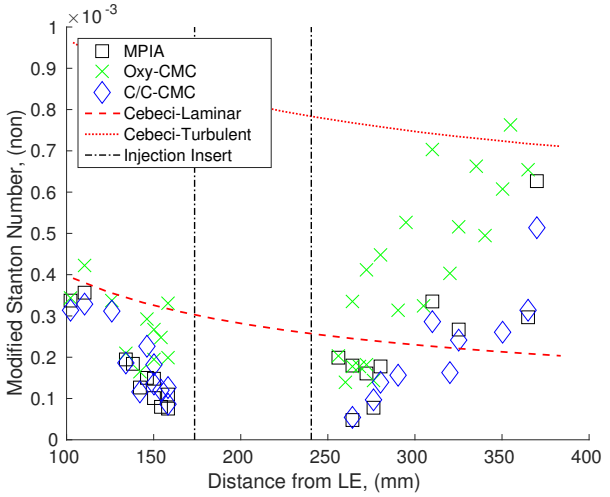

Figure 8. Comparison: laminar low mom. T4 shots in order: 11901, 11926, and 11903

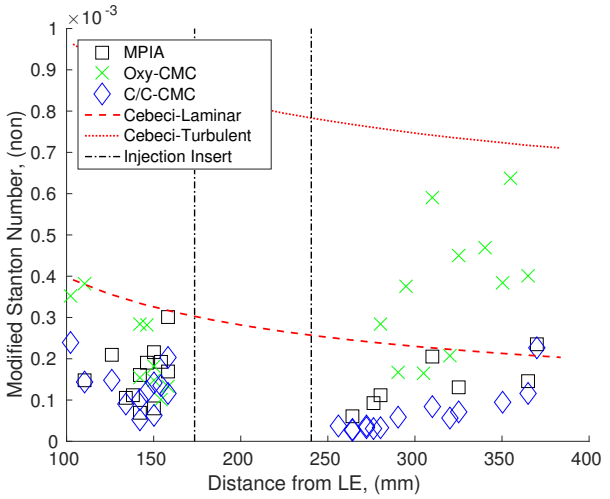

Figure 9. Comparison: laminar high mom. T4 shots in order: 11900, 11908, and 11902

from any of the injectors while effusing into the transitional-turbulent BL.

Turbulent - High Momentum

In Fig. 11, which compares the performance of all the injectors for the turbulent high-momentum case, the C/C has the largest cooling effect for the longest downstream-extent. Comparatively, the MPIA also cools to below the originally measured laminar level, as seen as the baseline in Fig. 5, but rises to a level closer to the theoretical laminar level by the end of the plate. It should also be noted that no separation is detectable in the THFG traces in front of the injectors for this case.

The oxy-CMC again performs the worst at cooling but interestingly produces a heat-transfer level lower than that seen for the high momentum injection into the laminar BL (Fig. 9). The exact mechanism for this difference is currently unknown but it is postulated that the interaction of the effusion fluid from the oxygen CMC has less of a destabilizing effect on the, thicker, forced-transition BL than the smaller laminar BL.

Conclusion

Overall, when comparing the three different injectors, the C/C

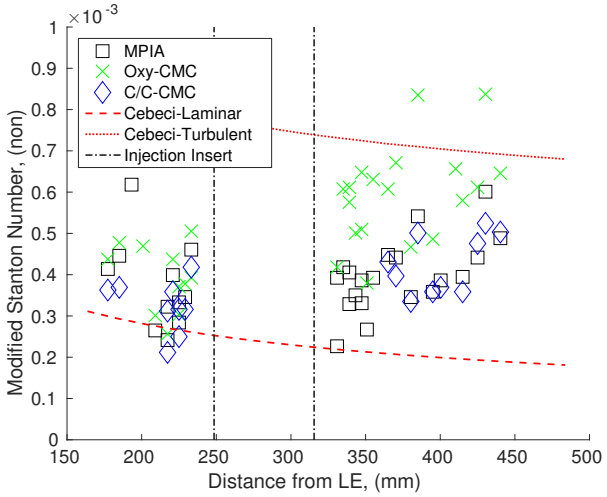

Figure 10. Comparison: transitional-turbulent low mom. T4 shots in order: 11920, 11927, and 11916

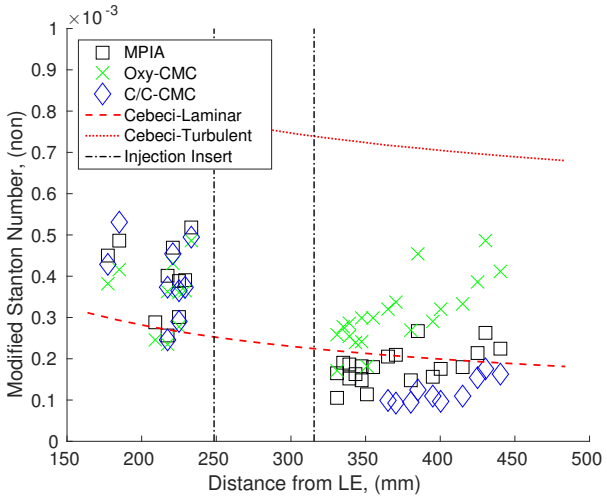

Figure 11. Comparison: transitional-turbulent high mom. T4 shots in order: 11919, 11921, and 11915

CMC performs the best, in that it achieves the greatest reduction in heat-transfer to the plate and also, achieves film-cooling for the longest downstream-extent for all the cases considered. The MPIA has a comparable performance for the low momentum injection cases but clearly does not perform as well for the high-momentum case. Both the MPIA and C/C achieve heat-transfer reductions below the laminar level for the forced transitional-turbulent high momentum case.

The oxygen compatible CMC injector rapidly transitions the BL for both the low and high momentum cases when injecting into a laminar BL. Also, this injector achieves a larger reduction in heat-transfer at the end of the sensor field for the turbulent high momentum case than for the laminar, the inverse trend to the other two injectors.

Finally, all of the injectors tested separate the BL in front of the injection location when injecting into a laminar BL and do not for the transitional-turbulent BL.

It is the authors' recommendation, from the preliminary results of this performance comparison study, that the C/C CMC be selected when looking for a distributed injection method on the inlet of a scramjet-powered vehicle.

Acknowledgements

This research was financially supported by the the Australian Research Council's Discovery Projects funding scheme (project number 120101009); the German Research Foundation (Deutsche Forschungsgemeinschaft – DFG) in the framework of the Sonderforschungsbereich Transregio 40; and the UQRS. Additional assistance was provided through the use of resources from the National Computational Infrastructure (NCI), which is supported by the Australian Government. The authors would also like to acknowledge the T4 tunnel support staff: Keith Hitchcock and Sam Grieve; and the T4 tunnel operators: Zac Denman, Will Landsberg, Augusto Fontan Moura, and Jens Kunze.

References

[1] Berry, S. A., Auslender, A. H., Dilley, A. D. and Calleja, J. F., Hypersonic boundary-layer trip development for Hyper-X, *Journal of Spacecraft and Rockets*, **38**, 2001, 853–864.

[2] Berry, S. A., Horvath, T. J., Hollis, B. R., Thompson, R. A. and Hamilton, H. H., X-33 Hypersonic Boundary-Layer Transition, *Journal of Spacecraft and Rockets*, **38**, 2001, 646–657.

[3] Boyce, R. R., Schramm, J. M., Oberg, D., Hannemann, K. and Brown, L., Shock tunnel and numerical studies of a large inlet-fuelled inward turning axisymmetric scramjet, in *18th AIAA/3AF International Space Planes and Hypersonic Systems and Technologies Conference*, 2012.

[4] Capra, B. R., Boyce, R. R., Kuhn, M. and Hald, H., Combustion enhancement in a scramjet engine using oxygen enrichment and porous fuel injection, *Journal of Fluid Mechanics*, **767**, 2015, 173–198.

[5] Cebeci, T. and Bradshaw, P., *Physical and Computational Aspects of Convective Heat Transfer*, Springer-Verlag, New York, NY, 1984.

[6] Heppenheimer, T. A., *Facing the Heat Barrier : A History of Hypersonics*, NASA, 2007.

[7] Lorrain, P., Brieschenk, S., Capra, B. and Boyce, R., A Detailed Investigation of Nominally 2-D Radical-Farming Scramjet Combustion, in *18th AIAA/3AF International Space Planes and Hypersonic Systems and Technologies Conference*, 2012.

[8] Pudsey, A. S., Boyce, R. R. and Wheatley, V., Hypersonic Viscous Drag Reduction via Multiporthole Injector Arrays, *JPP*, **29**, 2013, 1087–1096.

[9] Schetz, J. A. and Nerney, B., Turbulent Boundary Layer with Injection and Surface Roughness, *AIAA Journal*, **15**, 1977, 1288–1294.

[10] Schetz, J. A. and Overeem, J. V., Skin Friction Reduction by Injection Through Combinations of Slots and Porous Sections, *AIAA Journal*, **13**, 1975, 971–972.

[11] Selzer, M., Hald, H., Schweikert, S. and Wolfersdorf, J. V., Measurements of Surface Exhalation Characteristics of Porous Fibre Reinforced Composites, in *4th International Conference on Porous Media and its Applications in Science and Engineering*, 2012.

[12] Wise, D. J. and Smart, M. K., Roughness-Induced Transition of Hypervelocity Boundary Layers, *Journal of Spacecraft and Rockets*, **51**, 2014, 847–854.